A Generalization for Stable Mixed Finite Elements

Andrew Gillette
Department of Mathematics
University of Texas at Austin
agillette@math.utexas.edu

Chandrajit Bajaj
Department of Computer Sciences
University of Texas at Austin
bajaj@cs.utexas.edu

ABSTRACT

Mixed finite element methods solve a PDE involving two or more variables. In typical problems from electromagnetics and electrodiffusion, the degrees of freedom associated to the different variables are stored on both primal and dual domain meshes and a discrete Hodge star is used to transfer information between the meshes. We show through analysis and examples that the choice of discrete Hodge star is essential to the model and numerical stability of a finite element method. We also show how to define interpolation functions and discrete Hodge stars on dual meshes which can be used to create previously unconsidered mixed methods.

1. INTRODUCTION

The theory of Discrete Exterior Calculus has united many finite element methods into a common and canonical mathematical framework. We highlight three important conclusions of this theory:

1. Mixed finite element methods require degrees of freedom to be assigned to both primal and dual meshes of the same domain.

2. A discrete Hodge star is used to transfer information between primal and dual meshes.

3. Whitney elements provide stable finite elements for the primal mesh.

These conclusions raise two questions. First, how should a discrete Hodge star be defined in order to maintain the stability of a mixed method? Second, is it possible to provide stable finite elements for the dual mesh without transferring information to the primal mesh?

We demonstrate the importance of these issues via a problem from electromagnetics. Using a Discrete Exterior Calculus analysis of Maxwell's equations, one can derive a second order vector wave equation

$$\mathbb{D}_1(\mathbb{M}_1)^{-1}\mathbb{D}_1^T\vec{H} = \omega^2(\mathbb{M}_2)^{-1}\vec{H},$$

where $\vec{H}$ is a magnetic field intensity 1-form on the dual mesh, ω is a coefficient, $\mathbb{D}_1$ is a rectangular incidence matrix having entries of 0 and ± 1 only, and $\mathbb{M}_k$ is a square matrix representing the discretization of the Hodge star operator. Typically, $\mathbb{M}_k$ is defined so that it is a sparse matrix while its inverse $(\mathbb{M}_k)^{-1}$ is not sparse.

Both questions raised above are of interest in this example. First, the $\mathbb{M}_1$ and $\mathbb{M}_2$ matrices must be defined in such a way that the resulting finite element method is stable, a notion we will make precise later. Second, since computing the inverse of the $\mathbb{M}_k$ matrices threatens numerical stability and lengthens computational time, it would be useful to have an interpolant defined for the degrees of freedom of $\vec{H}$. We will show that such an interpolant can also be used to construct a sparse analogue of $(\mathbb{M}_k)^{-1}$ directly, i.e. without matrix inversion.

The main contributions of this paper are as follows:

- In Section 3, we use Natural Element Coordinate functions to define an interpolatory basis on polyhedral dual meshes in $\mathbb{R}^3$ and utilize them to define a discrete Hodge star $\mathbb{M}_k^{Dual}$ for use on dual meshes. This dual discrete Hodge star is sparse and thus obviates the typical practice of inverting large sparse discrete Hodge star matrices defined on primal simplicial meshes.

- In Section 4, we show that the choice of discrete Hodge star and its inverse are crucial to the model and numerical stability of mixed finite element methods. Our analysis and techniques use the generalized framework of deRham diagrams and Discrete Exterior Calculus, resulting in simple and universal stability criteria.

- In Section 5, we cast a variety of examples into our common notational framework and show how to formulate equivalent dual formulations of the problem from a DEC-based analysis. We analyze the stability of each formulation using the techniques developed in Sections 3 and 4.

We begin with a discussion of prior work and the notation necessary to fully describe the problems considered.

Permission to make digital or hard copies of all or part of this work for personal or classroom use is granted without fee provided that copies are not made or distributed for profit or commercial advantage and that copies bear this notice and the full citation on the first page. To copy otherwise, to republish, to post on servers or to redistribute to lists, requires prior specific permission and/or a fee.
2010 ACM Symposium of Solid and Physical Modeling (SPM '10), Haifa, Israel
Copyright 2010 ACM 978-1-60558-984-8/10/09 ...$10.00

2. PRIOR WORK AND NOTATION

Discrete Exterior Calculus (DEC) is an attempt to create from scratch a discrete theory of differential geometry and topology whose definitions and theorems mimic their continuous counterparts [12, 1]. A central conclusion of the theory is that degrees of freedom for finite elements should be assigned to mesh vertices, edges, faces or interiors according to the dimensionality of the variable being modeled. If these degrees of freedom have a natural geometric duality, as occurs for example between electric and magnetic fields, two meshes of the domain are necessary - a primal and dual mesh [11]. This has given rise to DEC-based methods for solving problems of Darcy flow [13], electromagnetism [10] and elasticity [22], among others.

The primal domain mesh of an n-manifold is a simplicial complex K. We denote k-simplices by σ^k where $0 \leq k \leq n$. The dual domain mesh $\star K$ is defined by taking the barycenters of n-simplices and connecting them based on simplex adjacency in the usual manner. We denote dual k-cells by $\star\sigma^k$. Note that $\star\sigma^k$ is an $(n-k)$-dimensional polytope and is associated to the k-dimensional simplex σ^k. The measure of σ^k (respectively $\star\sigma^{n-k}$) is denoted $|\sigma^k|$ (respectively $|\star\sigma^{n-k}|$), meaning length for $k=1$, area for $k=2$, and volume for $k=3$, with the convention that $|\sigma^0| = |\star\sigma^n| = 1$. Examples for $n=2$ are shown in Figure 1.

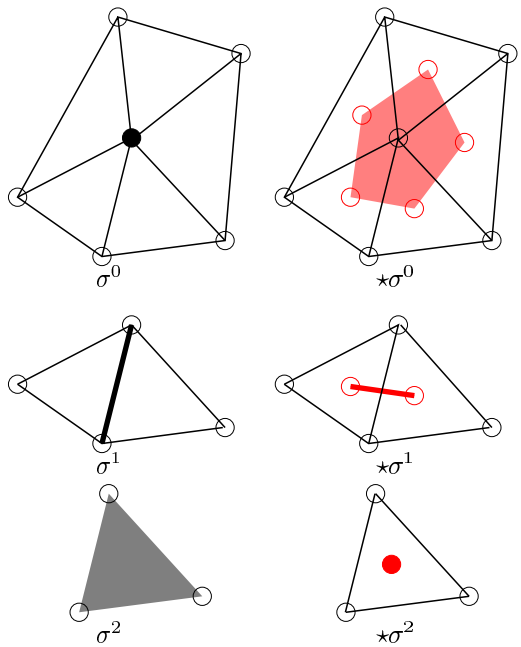

Figure 1: Primal simplices are shown in black on the left: σ^0 is a vertex, σ^1 is an edge, and σ^2 is a face. Their corresponding dual cells for $n=2$ are shown in red on the right: $\star\sigma^2$ is the barycenter of σ^2, $\star\sigma^1$ is an edge between barycenters, and $\star\sigma^0$ is a planar polygon with barycenters as vertices. In three dimensions ($n=3$), primal vertices have dual polytopes, primal edges have dual polygonal facets, primal faces have dual edges, and primal volumes have dual vertices.

Pertinent definitions from DEC theory are summarized by Figure 2 and described below. The vector space of k-cochains, i.e. linear mappings from k-simplices to $\mathbb{R}$, is denoted $\mathcal{C}^k$. This space is the discrete analogue of Λ^k, the space of differential k-forms on the domain. The exterior derivative map $d_k : \Lambda^k \to \Lambda^{k+1}$ is used to define the deRham complex:

$$\Lambda^0 \xrightarrow{d_0} \Lambda^1 \xrightarrow{d_1} \cdots \xrightarrow{d_{n-1}} \Lambda^n.$$

In this work, we will focus on problems in $\mathbb{R}^3$, in which the deRham complex becomes the more familiar sequence of finite element spaces and differential maps:

$$H^1 \xrightarrow{\text{grad}} H(\text{curl}) \xrightarrow{\text{curl}} H(\text{div}) \xrightarrow{\text{div}} L^2.$$

The interpolation map $\mathcal{I}_k : \mathcal{C}^k \to \Lambda^k$ converts k-cochains into k-forms with continuity prescribed by the deRham complex. We will use Whitney forms for these maps which were first described in [20] and later recognized by Bossavit [5] and others as the correct generalization of edge and face elements needed for DEC theory.

Whitney k-forms are piecewise linear functions on a primal mesh, one for each k-simplex in the mesh. The Whitney 0-form associated to a vertex $\sigma^0 := v_i$ is denoted

$$\eta_{\sigma^0} := \lambda_i,$$

where λ_i is the barycentric function for the vertex. More precisely, λ_i is defined by the condition of being linear on every simplex of the mesh, subject to the constraints $\lambda_i(v_j) = \delta_{ij}$. The Whitney 1-form associated to an oriented edge $\sigma^1 := [v_i, v_j]$ is the vector-valued function

$$\eta_{\sigma^1} := \lambda_i \nabla\lambda_j - \lambda_j \nabla\lambda_i.$$

The Whitney 2-form associated to an oriented face $\sigma^2 := [v_i, v_j, v_k]$ is the vector-valued function

$$\eta_{\sigma^2} := 2\left(\lambda_i \nabla\lambda_j \times \nabla\lambda_k + \lambda_j \nabla\lambda_k \times \nabla\lambda_i + \lambda_k \nabla\lambda_i \times \nabla\lambda_j\right)$$

The Whitney 3-form associated to an oriented tetrahedron σ^3 is its characteristic function, i.e.

$$\eta_{\sigma^3} := \chi_{\sigma^3} = \begin{cases} 1 & \text{on } \sigma^3 \\ 0 & \text{otherwise} \end{cases}$$

The Whitney interpolant $\mathcal{I}_k$ of a k-cochain ω, is

$$\mathcal{I}_k(\omega) := \sum_{\sigma^k \in \mathcal{C}_k} \omega(\sigma^k)\eta_{\sigma^k}. \tag{1}$$

It is evident from Figure 2 that the Whitney forms only map primal cochains to piecewise smooth functions, leaving open the possibility of analogous dual interpolatory functions. By this, we mean functions with some type of continuity defined uniquely by degrees of freedom associated to elements in a dual domain mesh.

The starting point for these types of functions comes from Wachspress [18] who developed generalized barycentric coordinates for convex polygons. Many extensions have come out of his work, as surveyed by Sukumar and Malsch in [17]. Christiansen has given an alternative approach based on a harmonic extension problem formulation [6]. In the context of DEC, the Sibson interpolant [16] is a natural choice as it produces non-negative nodal basis functions and reduces

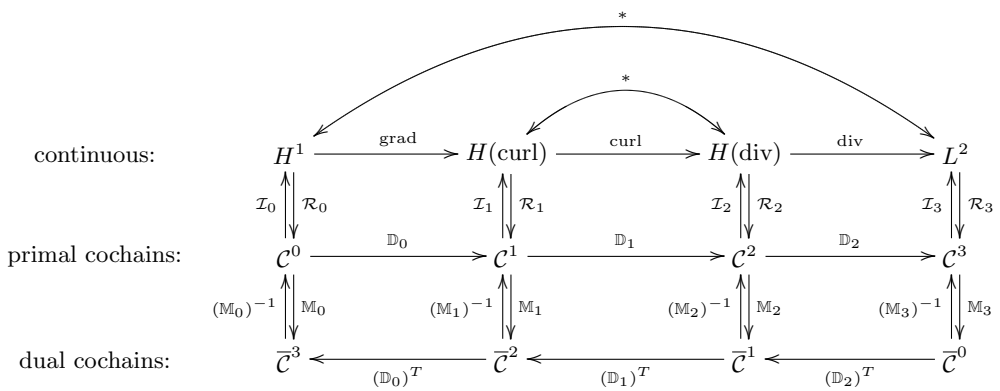

Figure 2: The combined DEC and deRham diagram for a contractible domain in $\mathbb{R}^3$.

to bilinear functions on rectangles. Accordingly, these functions have been called Natural Element Coordinates and we use a slight variant of them [15] to ensure a certain local dependence property, as discussed in Section 3.

Finally, we discuss the Hodge star operator and its discretization. As shown in Figure 2, the continuous Hodge star $*$ maps between forms of complementary dimensions. It is defined as the unique map $* : \Lambda^k \to \Lambda^{n-k}$ satisfying the property

$$\alpha \wedge *\beta = (\alpha, \beta)_{\Lambda^k}\, \mu, \quad \forall \alpha, \beta \in \Lambda^k, \tag{2}$$

where $\wedge$ denotes the wedge product, $(\cdot,\cdot)_{\Lambda^k}$ denotes the inner product on k-forms, and μ is the volume n-form on the domain.

A discrete Hodge star $\mathbb{M}$ maps not only between cochains of complementary dimensions but also between primal and dual meshes [11]. A wide variety of discrete Hodge stars have been proposed in the literature, many of which are useful in only specific contexts. We summarize some of the more general definitions here and cast them into a common notational framework to aid in their comparison.

Desbrun et al. [7] define a diagonal discrete Hodge star by

$$(\mathbb{M}_k^{Diag})_{ij} := \frac{|\star\sigma_i^k|}{|\sigma_i^k|}\delta_{ij}. \tag{3}$$

The definition of $\mathbb{M}_k^{Diag}$ fits nicely into DEC theory when the dual mesh is defined by taking circumcenters of the primal simplices. In practice, however, it is often desirable to use barycenters to define the dual mesh as this guarantees that σ^k will intersect $\star\sigma^k$ in the ambient space.

A correction factor for using barycenters instead of circumcenters is given by Auchmann and Kurz [2]. They derive a discrete Hodge star using Whitney interpolants to produce

$$(\mathbb{M}_k^{Geom})_{ij} := \alpha_{ij}\beta_{ij}\frac{k(n-k)+1}{N_k}\frac{|\star\sigma_i^k|}{|\sigma_j^k|},$$

where α_{ij} is a material parameter, possibly tensorial, β_{ij} is a measure of local deviation of the barycenter from the circumcenter, and N_k is the number of k-simplices in an n-simplex. Note that if the barycenter and circumcenter are the same, then $\beta_{ii} = 1$ and we have $(\mathbb{M}_1^{Geom})_{ii} = (\mathbb{M}_1^{Diag})_{ii}$ up to a constant multiple. We show an example of the computation of β_{ij} in Figure 3.

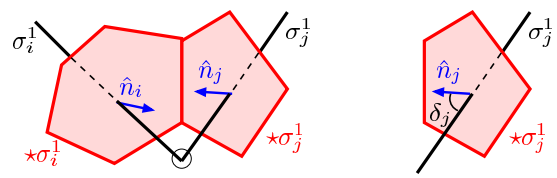

Figure 3: The deviation of the barycenter from the circumcenter for $n = 3$, $k = 1$ is $\beta_{ij} = \cos\gamma^{ij}/\cos\delta^j$ where γ^{ij} is the angle between the normals to the dual faces $\star\sigma_i^1$ and $\star\sigma_j^1$ (the vectors $\hat{n}_i$ and $\hat{n}_j$ on the left) and δ^j is the angle between the normal $\hat{n}$ of dual face $\star\sigma_j^1$ and the edge σ_j^1 (as shown on the right). Note that γ^{ii}=0. If the barycenter and circumcenter are identical, the dual face will be orthogonal and δ^j will be zero.

Wardetzsky and Wilson [19, 21] take a different approach, defining a combinatorial discrete Hodge star based on a discrete wedge product. Given a k-cochain ω^k and a j-cochain υ^j, they define their discrete wedge product to be

$$\omega^k \wedge \upsilon^j := \mathcal{R}_{k+j}(\mathcal{I}_k\omega^k \wedge \mathcal{I}_j\upsilon^j).$$

The combinatorial Hodge star is then defined implicitly by the relationship

$$\left(\mathbb{M}_k^{Comb}\omega^k, \upsilon^{n-k}\right)_{\mathcal{C}^{n-k}} = \sum_{\tau\in\mathcal{C}_n}(\mathcal{R}_n(\mathcal{I}_k\omega^k \wedge \mathcal{I}_{n-k}\upsilon^{n-k}))(\tau),$$

for all $\upsilon^{n-k} \in \mathcal{C}^{n-k}$. DiCarlo et al. [8] have recently described a discrete Hodge star by a similar method using metrized chains instead of cochains. Both approaches map primal k-cochains (or metrized chains) to *primal* $(n-k)$-cochains (or metrized chains) instead of dual $(n-k)$-cochains. This limits the applicability of the definition to certain types of problems and meshes, preventing it from being used in a generalized finite element method.

The approach closest to the finite difference roots of DEC theory was originally proposed by Dodziuk [9] and imple-

mented by Bell [3]. It uses Whitney interpolants explicitly to define matrix entries as

$$(\mathbb{M}_k^{Whit})_{ij} := \left(\eta_{\sigma_i^k}, \eta_{\sigma_j^k}\right) = \int_K \eta_{\sigma_i^k} \cdot \eta_{\sigma_j^k} \tag{4}$$

The inner product here is the standard integration of scalar or vector valued functions over the domain K. We note that no authors to our knowledge have defined a discrete Hodge star using dual interpolatory functions as we propose in this work.

3. DUAL WHITNEY INTERPOLANTS AND DUAL DISCRETE HODGE STARS

It is evident from the DEC-deRham diagram in Figure 2 that the direct interpolation of degrees of freedom on a dual mesh is not available in the common theory. Further, we have seen from the discussion in Section 2 that the definition of $(\mathbb{M}_k)^{-1}$ has only been implied from definitions of $\mathbb{M}_k$. In this section, we define a set of interpolation functions $\overline{\mathcal{I}}$ analogous to the Whitney interpolants defined in (1) and use them to provide an explicit definition of a dual discrete Hodge star.

Since Whitney forms on the primal mesh are defined using barycentric coordinate functions for simplices, it is natural to construct an interpolation function on the dual mesh using a generalized barycentric coordinate system. On a dual mesh, this entails a set of functions $\{\overline{\lambda}_i\}$, one for each vertex $\{v_i\}$ of the dual mesh, satisfying the following properties:

L1. Positivity: $0 \leq \overline{\lambda}_i \leq 1$

L2. Interpolation: $\overline{\lambda}_i(v_j) = \delta_{ij}$

L3. Partition of unity: $\sum_i \overline{\lambda}_i = 1$

L4. Linear completeness: $\sum_i v_i \overline{\lambda}_i(x) = x$

These properties can be achieved using a modification of the Natural Element Coordinate (NEC) functions which we now define. Given a polytope with vertices $\{v_i\}$ in $\mathbb{R}^n$, the first order Voronoi region of vertex i is those points in the domain which are closer to v_i than any other vertex v_j:

$$VR(v_i) := \{x \in \mathbb{R}^n : d(x, v_i) \leq d(x, v_j), \forall j \neq i\}.$$

Given a point p inside the polytope, the Vornonoi region formed by adding p to the vertex list is denoted

$$VR(p) := \{x \in \mathbb{R}^n : d(x, p) \leq d(x, v_i), \forall i\}.$$

Using $|\cdot|$ to denote the usual Lebesgue measure of a region (length for one-dimensional regions, area for two-dimensional regions, etc), the Natural Element Coordinate (NEC) of a point p with respect to vertex v_i is defined to be

$$\overline{\lambda}_i(p) := \frac{|VR(p) \cap VR(v_i)|}{|VR(p)|}$$

We show an example in Figure 4. The NEC functions are defined to be zero outside the polytope and have been shown to satisfy properties L1-L4 for convex polytopes. Further, they are C^∞ within each cell except at vertices where they are C^0 and at Voronoi spheres where they are C^1 [23]. The NEC functions generalize barycentric functions as it can be shown that $\overline{\lambda}_i \equiv \lambda_i$ on a simplex.

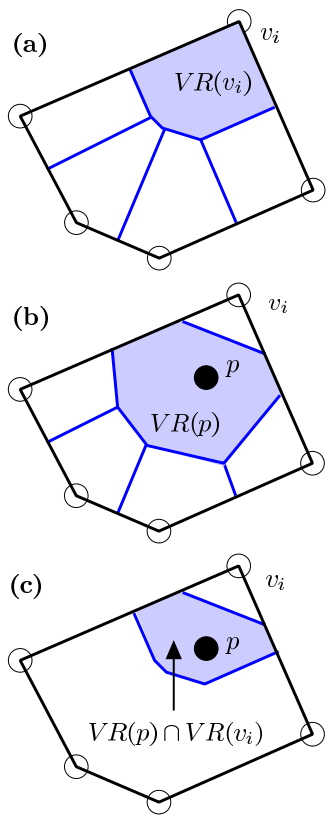

Figure 4: Geometric calculation of a NEC coordinate. (a) $VR(v_i)$ is the Voronoi region associated to vertex v_i in the polygon. (b) $VR(p)$ is the Voronoi region associated to p if it is added to the vertex list. (c) The quantity $|VR(p) \cap VR(v_i)|$ is exactly $|VR(p)|$ if $p = v_i$ and decays to zero as p moves away from v_i, with values identically zero at all vertices besides v_i. This analogue to barycentric coordinates makes the NEC functions suitable for use in dual interpolants.

Milbradt and Pick [15] modify the definition of NEC functions for concave polytopes so that an additional condition holds:

L5. Boundary agreement: If x lies on an edge (facet) and v_i is not a vertex of the edge (facet) then $\overline{\lambda}_i(x) = 0$.

In other words, the coordinates of a point on an edge or facet of the polytope are dependent only on the NEC functions associated to the boundary vertices of that edge or facet. This ensures C^0 conformity between adjacent mesh elements and allows us to define Whitney-like interpolants $\{\eta_{\star\sigma_i^k}\}$ on a dual mesh. The 0-form associated to a dual vertex $\star\sigma^3 := v_i$ is

$$\eta_{\star\sigma^3} := \overline{\lambda}_i,$$

the NEC function for the vertex. The 1-form associated to an oriented dual edge $\star\sigma^2 := [v_i, v_j]$ is the vector-valued function

$$\eta_{\star\sigma^2} := \overline{\lambda}_i \nabla \overline{\lambda}_j - \overline{\lambda}_j \nabla \overline{\lambda}_i$$

Assigning a vector-valued function to an oriented dual face is more subtle as the face is in general not a triangle. The dual face $\star\sigma^1$ will have m vertices where m is the number of tetrahedra σ^3 sharing the edge σ^1. To associate a single 2-form to the face, we take the vertices in groups of consecutive triples and average them:

$$\eta_{\star\sigma^1} := \frac{1}{m}\sum_{i=0}^{m-1}(\overline{\lambda}_i\nabla\overline{\lambda}_{i+1}\times\nabla\overline{\lambda}_{i+2}) + (\overline{\lambda}_{i+1}\nabla\overline{\lambda}_{i+2}\times\nabla\overline{\lambda}_i)$$

$$+(\overline{\lambda}_{i+2}\nabla\overline{\lambda}_i\times\nabla\overline{\lambda}_{i+1}),$$

where indices are taken mod m. The 3-form $\eta_{\star\sigma^0}$ associated to a dual cell $\star\sigma^0$ is its characteristic function:

$$\eta_{\star\sigma^0} := \chi_{\star\sigma^0} = \begin{cases} 1 & \text{on } \star\sigma^0 \\ 0 & \text{otherwise} \end{cases}$$

To compare our dual forms to primal Whitney forms, we state the three characteristic criteria of primal Whitney forms.

W1. **Partition of Unity.** Let $\mathbf{1}$ be the constant function with value 1 everywhere on the domain. Then

$$\sum_{\sigma^0\in K}\eta_{\sigma^0} = \mathbf{1} \quad \text{and} \quad \sum_{\sigma^3\in K}\eta_{\sigma^3} = \mathbf{1}.$$

Let $\mathbb{I}$ denote the 3×3 identity matrix. Let $\vec{\sigma}^1$ denote the vector in $\mathbb{R}^3$ with direction and length the same as σ^1. Let $\vec{\sigma}^2$ denote the vector in $\mathbb{R}^3$ with direction normal to σ^2 (based on the orientation of K) and magnitude equal to the area of σ^2. Then

$$\sum_{\sigma^1\in K}\vec{\sigma}^1.\eta_{\sigma^1} = \mathbb{I} \quad \text{and} \quad \sum_{\sigma^2\in K}\vec{\sigma}^2.\eta_{\sigma^2} = \mathbb{I}.$$

The "." operation denotes matrix multiplication between the 3×1 matrix $\vec{\sigma}^i$ and the 1×3 matrix η_{σ^i}.

W2. **Localization.** The support of η_{σ^k} is contained within the tetrahedra adjacent to σ^k.

W3. **Exactness.** For $k = 1, 2, 3$,

$$\text{im } \mathcal{I}_k\mathbb{D}_{k-1} \subseteq \ker d_k.$$

If the domain is contractible, the containment is an equality.

We now state a series of results showing that the dual Whitney forms satisfy the same properties.

LEMMA 1. ***Partition of Unity.*** *Property W1 holds if σ^k is replaced by $\star\sigma^{3-k}$.*

PROOF. Dual vertices are associated to the NEC functions which satisfy L3, a partition of unity property. Dual edges are associated to direct analogues of Whitney 1-forms using NEC functions instead of barycentric functions. The proof that the Whitney 1-forms satisfy a partition of unity property only uses the properties L1-L5 for barycentric functions. Thus it carries through to NEC coordinates. A similar argument holds for dual faces. Dual cells are associated to characteristic functions and thus satisfy the partition of unity property trivially. □

LEMMA 2. ***Localization.*** *The support of $\eta_{\star\sigma^k}$ is contained within the dual cells adjacent to σ^k.*

PROOF. This follows directly from the fact that the NEC coordinates, like the barycentric coordinates, satisfy the localization property. □

LEMMA 3. ***Exactness.*** *For $k = 0, 1, 2$,*

$$im\ \overline{\mathcal{I}}_{3-k}(\mathbb{D}_k)^T \subseteq \ker d_k.$$

If the domain is contractible, the containment is an equality.

PROOF. The proof that Whitney forms satisfy the exactness property only uses the properties L1-L5 for barycentric functions and the fact that $\mathbb{D}_k$ is the transpose of the incidence matrix for k-simplices. Thus, the proof carries through to the dual formulation of the property. □

We define the dual Whitney interpolant of a dual $(n-k)$-cochain $\overline{\omega}\in\overline{\mathcal{C}}^{n-k}$ to be

$$\overline{\mathcal{I}}_{n-k}(\overline{\omega}) := \sum_{\star\sigma^k\in\overline{\mathcal{C}}_{n-k}}\overline{\omega}(\star\sigma^k)\eta_{\star\sigma^k}. \tag{5}$$

We use the dual interpolants to define a dual discrete Hodge star by

$$((\mathbb{M}_k^{Dual})^{-1})_{ij} := \left(\eta_{\star\sigma_i^k}, \eta_{\star\sigma_j^k}\right). \tag{6}$$

The inner product here is the standard integration of scalar or vector valued functions over the dual domain $\star K$. For instance, in the case $k = 3$, we have

$$((\mathbb{M}_3^{Dual})^{-1})_{ij} := \left(\eta_{\star\sigma_i^3}, \eta_{\star\sigma_j^3}\right) = \int_{\star K}\overline{\lambda}_i\overline{\lambda}_j.$$

The formulation for other k values will similarly involve integrals of the $\overline{\lambda}_i$ functions.

LEMMA 4. *$(\mathbb{M}_k^{Dual})^{-1}$ is sparse.*

PROOF. By Lemma 2, $\eta_{\star\sigma^k}$ has localized support. Entry ij of $(\mathbb{M}_k^{Dual})^{-1}$ will be non-zero only if $\star\sigma_i^k$ and $\star\sigma_j^k$ are adjacent. Thus each row of the matrix will have at most as many non-zero entries as $\star\sigma_i^k$ has adjacent $n-k$ cells, meaning the matrix is sparse. □

Lemma 4 does not hold if $\mathbb{M}_k^{Dual}$ is replaced by $\mathbb{M}_k^{Geom}$, $\mathbb{M}_k^{Comb}$, or $\mathbb{M}_k^{Whit}$ as these sparse matrices typically have dense inverses. We note that $(\mathbb{M}_k^{Diag})^{-1}$ is trivially sparse since it is diagonal. However, as we will show in Section 4, $\mathbb{M}_k^{Diag}$ is lacking in both model and numerical stability. Hence, $\mathbb{M}_k^{Dual}$ is a novel and robust option for computing an inverse discrete Hodge star.

4. STABILITY CRITERIA FROM DISCRETE HODGE STARS

Three types of stability criteria must be considered when designing a finite element method. First, the discrete solution computed by the method should belong to a subspace of the

solution space to the continuous problem; we call this *model stability* or discretization conformity. Second, the true error between the discrete and continuous solutions should be bounded by a multiple of the best approximation error; this is the classical finite element notion of *discretization stability*. Third, accumulated numerical errors due to machine precision should not compromise the computed solution; we call this *numerical stability* or bounded roundoff error. In this paper, we focus on model and numerical stability and how they are affected by the type of discrete Hodge star operator $\mathbb{M}_k$ used in the method.

Previous stability criteria for $\mathbb{M}_k$ focus on properties of the matrix itself. In particular, it is common to seek a definition of $\mathbb{M}_k$ so that it is a sparse, symmetric, and positive definite matrix. Requiring $\mathbb{M}_k$ to be symmetric and positive definite is equivalent to saying $\mathbb{M}_k$ has only positive eigenvalues. This avoids computing imaginary solutions with no physical meaning and is necessary for $\mathbb{M}_k$ to agree with the inner product structure on the space. Our contention is that these criteria alone are not sufficient for evaluating the stability of a method as we explain below.

4.1 Model Stability

To maintain the model stability of a finite element method, a discrete Hodge star $\mathbb{M}_k$ should aim to make the following diagram commutative:

$$\begin{tikzcd}
\text{continuous} & \Lambda^k \arrow[r, leftrightarrow, "*"] \arrow[d, shift left, "\mathcal{R}_k"] & \Lambda^{n-k} \arrow[d, shift left, "\overline{\mathcal{R}}_{n-k}"] & \text{continuous} \\
\text{primal} & \mathcal{C}^k \arrow[r, shift left, "\mathbb{M}_k"] \arrow[u, shift left, "\mathcal{I}_k"] & \overline{\mathcal{C}}^{n-k} \arrow[l, shift left, "(\mathbb{M}_k)^{-1}"] \arrow[u, shift left, "\overline{\mathcal{I}}_{n-k}"] & \text{dual}
\end{tikzcd}$$

No discrete Hodge star can satisfy this condition in its entirety as $\mathcal{R}$ (the deRham map) and $\mathcal{I}$ are not true inverses. Thus, we break the diagram down into different subcommutativity conditions:

- Commutativity at $\mathcal{C}^k$: $*\mathcal{I}_k = \overline{\mathcal{I}}_{n-k}\mathbb{M}_k$
- Commutativity at $\overline{\mathcal{C}}^{n-k}$: $*\overline{\mathcal{I}}_{n-k} = \mathcal{I}_k(\mathbb{M}_k)^{-1}$
- Commutativity at Λ^k: $\mathbb{M}_k\mathcal{R}_k = \overline{\mathcal{R}}_{n-k}*$
- Commutativity at Λ^{n-k}: $(\mathbb{M}_k)^{-1}\overline{\mathcal{R}}_{n-k} = \mathcal{R}_k*$

We focus on commutativity at $\mathcal{C}^k$ as an illustrative example. At the very least, one would hope to satisfy the condition in an integral sense, leading us to define **weak commutativity at $\mathcal{C}^k$** by the condition

$$\int_K \alpha \wedge *\mathcal{I}_k = \int_K \alpha \wedge \overline{\mathcal{I}}_{n-k}\mathbb{M}_k, \quad \forall \alpha \in \Lambda^k. \tag{7}$$

The definition of the Hodge star in (2) allows us to re-write the left side, yielding

$$\int_K (\alpha, \mathcal{I}_k)_{\Lambda^k}\mu = \int_K \alpha \wedge \overline{\mathcal{I}}_{n-k}\mathbb{M}_k, \quad \forall \alpha \in \Lambda^k. \tag{8}$$

We can use this criteria to prove model stability results such as the following.

Lemma 5. *For $n = 3$, $\mathbb{M}_0^{Whit}$ exhibits more model stability than $\mathbb{M}_0^{Diag}$*

Proof. We evaluate the weak commutativity at $\mathcal{C}^0$ condition on the basis cochain ω_i^0, defined to have value 1 on vertex σ_i^0 and value 0 on all other vertices. Using the definition of $\mathcal{I}_0$ from (1), we write

$$\left(\alpha, \mathcal{I}_0\left(\omega_i^0\right)\right)_{\Lambda^0} = (\alpha, \eta_{\sigma_i^0})_{H^1} = (\alpha, \lambda_i)_{H^1}$$

We evaluate the right side of (8) using the definition of $\overline{\mathcal{I}}_3$ from (5) and two different discrete Hodge stars. Using $\mathbb{M}_0^{Diag}$ from (3), we get

$$\begin{aligned}
\overline{\mathcal{I}}_3\mathbb{M}_0^{Diag}(\omega_i^0) &= \sum_{\star\sigma_j^0 \in \overline{\mathcal{C}}^3} (\mathbb{M}_0^{Diag}\omega_i^0)\chi_{\star\sigma_j^0}\mu \\
&= |\star\sigma_i^0|\chi_{\star\sigma_i^0}\mu
\end{aligned}$$

Hence the weak commutativity condition (8) in this case is

$$|K|(\alpha, \lambda_i)_{H^1} = \left|\star\sigma_i^0\right| \int_{\star\sigma_i^0} \alpha\mu, \quad \forall \alpha \in H^1. \tag{9}$$

If $\mathbb{M}_0^{Whit}$ from (4) is used instead, we have

$$\begin{aligned}
\overline{\mathcal{I}}_3\mathbb{M}_0^{Whit}(\omega_i^0) &= \sum_{\star\sigma_j^0 \in \overline{\mathcal{C}}^3} (\mathbb{M}_0^{Whit}\omega_i^0)\chi_{\star\sigma_j^0}\mu \\
&= \sum_j (\lambda_i, \lambda_j)\, \chi_{\star\sigma_j^0}.
\end{aligned}$$

In this case, the weak commutativity condition is

$$|K|(\alpha, \lambda_i)_{H^1} = \sum_j (\lambda_i, \lambda_j) \int_{\star\sigma_j^0} \alpha\mu, \quad \forall \alpha \in H^1. \tag{10}$$

Between (9) and (10), the former is a coarser approximation of the inner product $(\alpha, \lambda_i)_{H^1}$ and therefore is more likely to introduce error than the latter. □

Initial examinations of alternate scenarios of the commutativity conditions produce similar conclusions about the superiority of the Whitney-based discrete Hodge star. We plan to expand on this analysis in future work.

4.2 Local Structure of Discrete Hodge Stars

The continuous Hodge star $*$ is a local operator meaning its effect on a differential form evaluated at a particular point on a manifold depends only on the geometry of a local neighborhood of the point. The discrete Hodge star is thus required to be a local operator as well meaning the evaluation of $\mathbb{M}_k$ on a basis cochain ω_i^k (1 on σ_i^k and 0 otherwise) should involve values on only a few simplices adjacent to σ_i^k. In the language of matrix theory, this requirement says $\mathbb{M}_k$ should be sparse.

All the discrete Hodge stars considered in this paper - $\mathbb{M}_k^{Diag}$, $\mathbb{M}_k^{Geom}$, $\mathbb{M}_k^{Whit}$ and our dual discrete Hodge $(\mathbb{M}_k^{Dual})^{-1}$ - are sparse matrices by the nature of their respective definitions. In the case of $\mathbb{M}_k^{Whit}$, we prove a more specific characterization of the matrix's structure.

Lemma 6. *Entry ij in $\mathbb{M}_k^{Whit}$ is non-zero only if there exists $\sigma^n \in K$ such that σ^n has at least one vertex from σ_i^k and one vertex from σ_j^k.*

PROOF. Computing entry ij in $\mathbb{M}_k^{Whit}$ involves [4] summing terms of the form

$$\left(\int_K \lambda_1\lambda_2\right) \det\left(V_I^T W_J\right) \tag{11}$$

where λ_1, λ_2 are barycentric functions associated to $v_1 \in \sigma_i^k$, $v_2 \in \sigma_j^k$, respectively; I is a list of k vertices from σ_i^k not including v_1; J is a list of k vertices from σ_j^k not including v_2; and V_I, W_J are $n \times k$ matrices. The pth column of V_I is the vector $\nabla\lambda_p$ where λ_p is the barycentric function associated to the pth entry in I. The qth column of W_J is the vector $\nabla\lambda_q$ where λ_q is the barycentric function associated to the qth entry in J.

Observe that the support of the barycentric function associated to vertex v is contained within the n-simplices touching v. Thus, if there is no σ^n with at least one vertex from σ_i^k and one vertex from σ_j^k, the λ_1 and λ_2 appearing in (11) will always have disjoint support, making the entry zero. □

Using the same kind of reasoning, we have a similar result for our dual discrete Hodge star.

LEMMA 7. *Entry ij in $(\mathbb{M}_k^{Dual})^{-1}$ is non-zero only if there exists $\star\sigma^0 \in \star K$ such that $\star\sigma^0$ has at least one vertex from $\star\sigma_i^k$ and one vertex from $\star\sigma_j^k$.*

COROLLARY 1. *Let N_k denote the number of k-simplices in an n-simplex and let $A(\sigma^k)$ denote the number of n-simplices in K incident on at least one vertex from σ^k. Then the number of non-zero entries in row i of $\mathbb{M}_k^{Whit}$ or row i of $(\mathbb{M}_k^{Dual})^{-1}$ is at most $N_k A(\sigma_i^k)$.*

The bound can be sharpened for particular choices of n and k or if additional assumptions are made about K. As stated, however, the corollary provides a simple means for evaluating the computational expense of a particular discretization scheme as we will discuss in Section 5.

4.3 Numerical Stability

Many finite element methods require inverting $\mathbb{M}_k$ for some k in order to compute the solution. Hence, to maintain the numerical stability of a finite element method, the discrete Hodge star matrix should have a bounded condition number. Put differently, the entries of the matrix should be roughly the same order of magnitude. This requirement is frequently considered from the context of numerical analysis but is often absent from the literature on discrete operators.

The common thread in the geometrically-defined discrete Hodge stars $\mathbb{M}_k^{Diag}$ and $\mathbb{M}_k^{Geom}$ is a measurement of the size of dual cells i.e. $|\star\sigma^k|$. This suggests that geometric criteria on primal elements alone will not be sufficient to control the condition number of the discrete Hodge star matrix. In particular, since ratios of primal to dual cells are computed, we must satisfy the following criteria:

N1. Primal simplices σ^k satisfy geometric quality measures.

N2. Dual cells $\star\sigma^k$ satisfy geometric quality measures.

N3. The value of $|\star\sigma^k|/|\sigma^k|$ is bounded above and below.

N4. The primal and dual meshes do not have large gradation of elements, i.e. $\min_i |\sigma_i^k|$ and $\max_i |\sigma_i^k|$ are the same order of magnitude and $\min_i |\star\sigma_i^k|$ and $\max_i |\sigma_i^k|$ are the same order of magnitude.

Conditions N1 and N2 are required for discretization stability. Aspect ratio is often used as a geometric quality measure for tetrahedra. Conditions N3 and N4 are based on our analysis above. Condition N4 particular shows that these discrete Hodge stars are not fit for use on meshes tailored to multi-resolution situations where gradation is necessary to achieve reasonable computation times. We show some examples in Figures 5 and 6.

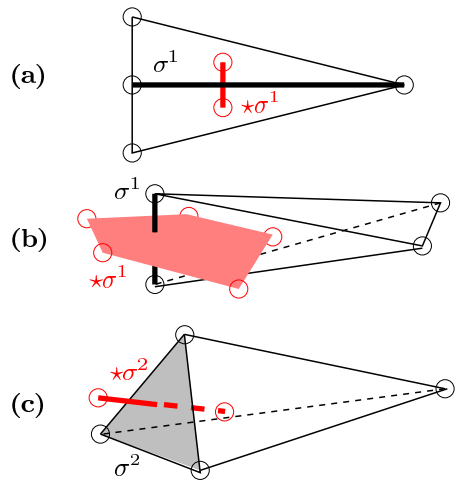

Figure 5: Examples illustrating how the measure of a primal simplex σ^k (black) and its dual $\star\sigma^k$ (red) need not be the same order of magnitude. (a) In this 2D example, the ratio $|\star\sigma^1|/|\sigma^1|$ can be made arbitrarily small by increasing the length of σ^1. (b) The ratio $|\star\sigma^1|/|\sigma^1|$ can be made arbitrarily large by decreasing the length of σ^1. (c) The ratio $|\star\sigma^2|/|\sigma^2|$ can be made arbitrarily large by decreasing the area of σ^2. Thus, a discrete Hodge star involving terms of the form $|\star\sigma^k|/|\sigma^k|$ may have a bad condition number unless primal *and* dual mesh quality is controlled.

For $\mathbb{M}_k^{Whit}$, the size of the matrix entries are controlled by the size of the inner products of Whitney basis forms. The integrals in (11) are on the order of the size of $|\sigma_k|$, meaning again that a large gradation in primal mesh element size could produce large condition numbers and hence numerical instability. Since it does not involve the size of dual mesh elements, however, $\mathbb{M}_k^{Whit}$ is more numerically stable against violations of conditions N2 and N3. Analogously, $(\mathbb{M}_k^{Dual})^{-1}$ is more numerically stable against violations of conditions N1 and N3. We summarize our conclusions below.

- $\mathbb{M}_k^{Diag}$ and $\mathbb{M}_k^{Geom}$ may produce numerical instability if any of conditions N1-N4 are not satisfied.
- $\mathbb{M}_k^{Whit}$ may produce numerical instability if conditions N1 or N4 are not satisfied.

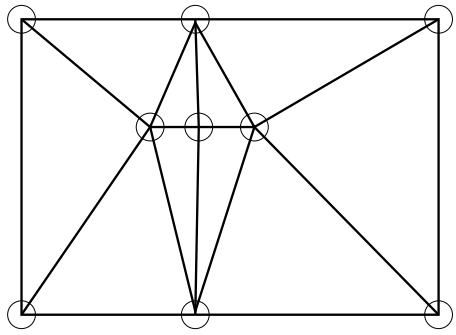

Figure 6: Graded meshes also present a problem for discrete Hodge stars involving primal-dual size ratios. The primal mesh shown here induces a wide variation in values of $|\star\sigma^k|/|\sigma^k|$ for $k = 0, 1, 2$. This can cause ill-conditioned $\mathbb{M}_k$ matrices, resulting in numerical instability.

- $(\mathbb{M}_k^{Dual})^{-1}$ may produce numerical instability if conditions N2 or N4 are not satisfied

5. APPLICATIONS

The dual interpolation functions $\overline{\mathcal{I}}_{n-k}$ we defined in (5) and the dual discrete Hodge star we defined in (6) are new tools for designing stable finite element methods. We now examine a variety of finite element problems from the literature and show how these tools coupled with the stability criteria we formulated in Section 4 can be used to derive alternative stable finite element discretizations.

5.1 Poisson Problem

The smooth Poisson problem on a domain $\Omega \subset \mathbb{R}^3$ is

$$\begin{cases} \Delta u &= f \quad \text{in } \Omega \\ \dfrac{\partial u}{\partial n} &= 0 \quad \text{on } \partial\Omega \end{cases}$$

The system is discretized by Bell [3] as

$$\mathbb{D}_0^T \mathbb{M}_1^{Whit} \mathbb{D}_0 u = f$$

where $u \in \mathcal{C}^0$, i.e. a vector of values at vertices of a primal mesh. This approach uses the following subset of the DEC-deRham diagram (Figure 2):

$$\begin{tikzcd} \text{primal:} & u \arrow[r, "\mathbb{D}_0"] & \mathbb{D}_0 u \arrow[d, "\mathbb{M}_1"] \\ \text{dual:} & (\mathbb{D}_0)^T \mathbb{M}_1 \mathbb{D}_0 u & \mathbb{M}_1 \mathbb{D}_0 u \arrow[l, "(\mathbb{D}_0)^T"'] \end{tikzcd}$$

The essential property of u is that it is a 0-form, not that it must be discretized as a primal 0-cochain. If we discretize it instead as a dual 0-cochain, we get a different portion of the DEC-deRham diagram:

$$\begin{tikzcd} \text{primal:} & (\mathbb{M}_2)^{-1}(\mathbb{D}_2)^T u \arrow[r, "\mathbb{D}_2"] & \mathbb{D}_2(\mathbb{M}_2)^{-1}(\mathbb{D}_2)^T u \\ \text{dual:} & (\mathbb{D}_2)^T u \arrow[u, "(\mathbb{M}_2)^{-1}"] & u \arrow[l, "(\mathbb{D}_2)^T"] \end{tikzcd}$$

Under this formulation, we can solve for u using the linear system

$$\mathbb{D}_2(\mathbb{M}_2^{Dual})^{-1}(\mathbb{D}_2)^T u = f.$$

By Lemma 4, $(\mathbb{M}_2^{Dual})^{-1}$ is sparse meaning this system is no more computationally expensive than the primal formulation using the sparse matrix $\mathbb{M}_1^{Whit}$. However, the dual-based system often requires many fewer computations than the primal-based system. To see this, define

$$\mathbb{A} := \mathbb{D}_0^T \mathbb{M}_1^{Whit} \mathbb{D}_0 \quad \text{and} \quad \mathbb{B} := \mathbb{D}_2(\mathbb{M}_2^{Dual})^{-1}(\mathbb{D}_2)^T.$$

Observe first that $\mathbb{A}$ is a $q_0 \times q_0$ matrix while $\mathbb{B}$ is a $q_2 \times q_2$ matrix where q_k denotes the number of k-simplices in the *primal* mesh. Thus, if a mesh has many more vertices than tetrahedra, $\mathbb{B}$ is a much smaller but equally powerful discretization of the problem.

Further, let a_{ij}, d_{ij}, m_{ij} denote the entries in the ith row and jth column of $\mathbb{A}$, $\mathbb{D}_k$ and $\mathbb{M}_1^{Whit}$, respectively. Multiplying out the matrices in $\mathbb{A}$, we find that

$$a_{ij} = \sum_{r,s=1}^{n} d_{si} d_{rj} m_{sr}.$$

In words, the value of a_{ij} depends on, possibly, all of the entries of $\mathbb{M}_1^{Whit}$ but only on the i and jth columns of $\mathbb{D}_0$. Since $\mathbb{M}_1^{Whit}$ is sparse, the number of summands used to compute a_{ij} is on the order of the number of tetrahedra which have both σ_i^0 and σ_j^0 as vertices. For a mesh with many tetrahedra grouped around certain edges, this may be very large.

By a similar analysis, we can show that the number of summands used to compute entry ij of $\mathbb{B}$ is on the order of the number of tetrahedra which have both σ_i^2 and σ_j^2 as faces, i.e. exactly two. Hence, we conclude that for meshes with many vertices of high incidence, the dual formulation requires fewer computations than the primal formulation and hence is less likely to accrue numerical errors.

We conclude that $(\mathbb{M}_2^{Dual})^{-1}$ provides a new dual formulation for Poisson's equation. We analyze this dual formulation for its numerical stability properties in comparison to the primal in the full version of this paper.

5.2 Maxwell's Equations

The curl equations derived from Maxwell's equations are

$$\nabla \frac{1}{\mu} \times \nabla \times \vec{E} = \omega^2 \epsilon \vec{E}$$

$$\nabla \frac{1}{\epsilon} \times \nabla \times \vec{h} = \omega^2 \vec{H}$$

where $\vec{E}$ and $\vec{H}$ are electric and magnetic field intensity, respectively, and μ and ϵ are constants. He and Teixeira [10] discretize these equations as

$$\mathbb{D}_1^T \mathbb{M}_2^{Whit} \mathbb{D}_1 \vec{E} = \omega^2 \mathbb{M}_1^{Whit} \vec{E}$$

$$\mathbb{D}_1 (\mathbb{M}_1^{Whit})^{-1} \mathbb{D}_1^T \vec{H} = \omega^2 (\mathbb{M}_2^{Whit})^{-1} \vec{H},$$

which they correctly identify as corresponding to primal and dual formulations of the problem. The subset of the DEC-

deRham diagram (Figure 2) used in these formulations is

$$\begin{array}{lccc} \text{primal:} & \vec{E} & \xrightarrow{\mathbb{D}_1} & \mathcal{C}^2 \\ & (\mathbb{M}_1)^{-1} \Big\uparrow\Big\downarrow \mathbb{M}_1 & & (\mathbb{M}_2)^{-1} \Big\uparrow\Big\downarrow \mathbb{M}_2 \\ \text{dual:} & \overline{\mathcal{C}}^2 & \xleftarrow[(\mathbb{D}_1)^T]{} & \vec{H} \end{array}$$

Here, the dual formulation of the problem is undesirable due to the necessity of computing the inverses of large sparse matrices. In particular $\mathbb{M}_k^{Whit}$ is a $q_k \times q_k$ sparse matrix where q_k is the number of k-simplices in the primal mesh. Hence, $(\mathbb{M}_k^{Whit})^{-1}$ may be a full rank $q_k \times q_k$ matrix requiring $O(q_k^2)$ computations, which is certainly undesirable for large scale applications. Using our dual discrete Hodge star, we recognize

$$\mathbb{D}_1(\mathbb{M}_1^{Dual})^{-1}\mathbb{D}_1^T\vec{H} = \omega^2(\mathbb{M}_2^{Dual})^{-1}\vec{H}$$

as an equivalent formulation of the dual problem. By Lemma 4, $(\mathbb{M}_k^{Dual})^{-1}$ is sparse meaning the requisite number of computations is closer to $O(q_k)$. Thus, $(\mathbb{M}_k^{Dual})^{-1}$ may provide a more numerically stable dual formulation of the problem.

5.3 Darcy Flow

The Darcy flow problem in $\mathbb{R}^3$ is formulated by Hirani et al. in [13] as

$$\begin{cases} \vec{f} + \frac{k}{\mu}\nabla p &= 0 \quad \text{in } \Omega, \\ \text{div}\vec{f} &= \phi \quad \text{in } \Omega, \\ \vec{f}\cdot\hat{n} &= \psi \quad \text{on } \partial\Omega, \end{cases}$$

where k and μ are constants. It is assumed that there is no external body force, the boundary $\Gamma := \partial\Omega$ is piecewise smooth, and the compatibility condition $\int_\Omega \phi d\Omega = \int_{\partial\Omega} \psi d\Gamma$ is satisfied. The system is discretized as

$$\begin{bmatrix} -(\mu/k)\mathbb{M}_2^{Diag} & \mathbb{D}_2^T \\ \mathbb{D}_2 & 0 \end{bmatrix} \begin{bmatrix} \vec{f} \\ p \end{bmatrix} = \begin{bmatrix} 0 \\ \phi \end{bmatrix}. \tag{12}$$

where $\vec{f} \in \mathcal{C}^2$ represents the volumetric flux through faces of the primal mesh and $p \in \overline{\mathcal{C}}^0$ represents the pressure at vertices of the dual mesh. We call this the **primal flux formulation**. The authors weight the entries of $\mathbb{M}_2^{Diag}$ with permeability coefficients in case permeability differs between adjacent tetrahedra. The authors interpolate the flux data by $\mathcal{I}_2\vec{f}$ and the pressure data by $\mathcal{I}_0(\mathbb{M}_3^{Diag})^{-1}p$. Thus, the subset of the DEC-deRham diagram (Figure 2) required for the primal flux formulation is

$$\begin{array}{lccc} \text{primal:} & \vec{f} & \xrightarrow{\mathbb{D}_2} & \mathbb{D}_2\vec{f} \\ & \Big\downarrow \mathbb{M}_2^{Diag} & & \\ \text{dual:} & \mathbb{M}_2^{Diag}\vec{f} & & \\ & (\mathbb{D}_2)^T p & \xleftarrow[(\mathbb{D}_2)^T]{} & p \end{array}$$

While flux ought to be valued over 2D faces, it need not be valued on primal mesh elements. Hence, we derive a **dual flux formulation** by treating flux $\vec{f}$ as an element of $\overline{\mathcal{C}}^2$ and pressure p as an element of $\mathcal{C}^0$. We use the sparse dual Hodge star $(\mathbb{M}_1^{Dual})^{-1}$ to transfer information from dual faces to primal edges. The flux data is interpolated by our dual interpolant $\overline{\mathcal{I}}_2\vec{f}$ and the pressure data by $\mathcal{I}_0 p$. The subset of the DEC-deRham diagram required for this new dual flux formulation is

$$\begin{array}{lccc} \text{primal:} & p & \xrightarrow{\mathbb{D}_0} & \mathbb{D}_0 p \\ & & & (\mathbb{M}_1^{Dual})^{-1}\vec{f} \\ & & & \Big\uparrow (\mathbb{M}_1^{Dual})^{-1} \\ \text{dual:} & (\mathbb{D}_0)^T\vec{f} & \xleftarrow[(\mathbb{D}_0)^T]{} & \vec{f} \end{array}$$

As discussed in Section 4, $\mathbb{M}_k^{Diag}$ does not provide for a stable discrete Hodge star since it lacks the subcommutativity conditions and may have a bad condition number. Thus, a more stable approach would be provided by the dual flux formulation as stated above or by using a different discrete Hodge star in the primal flux formulation, such as $\mathbb{M}_2^{Whit}$.

5.4 Electrodiffusion

We now consider a more elaborate example for which mixed finite element methods will be both necessary and complicated. The electrodiffusion equations govern the spatial distribution of electric potential and multiple ion species (indexed by k) in and near neuronal cells. They are formulated by Lopreore et. al [14] as

$$\begin{cases} \vec{J}_k &= -\left(\nabla c_k + \dfrac{Fz_k}{RT}c_k\vec{E}\right), \\ 0 &= \text{div}\left(\epsilon\vec{E}\right) + \displaystyle\sum_k c_k z_k F, \\ \vec{E} &= \nabla\phi, \\ 0 &= \dfrac{\partial}{\partial t}c_k + D_k \text{div } \vec{J}_k, \end{cases}$$

The variables in the problem are the electric potential ϕ, the electric field $\vec{E}$, the flux of the kth ion species $\vec{J}_k$, and the concentration of the kth ion species c_k. The physical and biological parameters F, z_k, R, T, ϵ, and D_k are assumed to be known constants for the purpose of our discussion.

A variety of schemes can be designed to solve the PDE, depending on what load data and boundary conditions are assumed. For instance, by taking the divergence of the first equation and some substitution, we can reduce to the set of just two equations

$$\begin{cases} 0 &= \text{div}\left(\epsilon\nabla\phi\right) + \displaystyle\sum_k c_k z_k F, \\ \dfrac{\partial}{\partial t}c_k &= D_k\Delta c_k + \dfrac{Fz_k}{RT}\text{div}(c_k\nabla\phi). \end{cases} \tag{13}$$

The top equation has been analyzed in Section 5.1. The bottom equation is time dependent and thus can be discretized using a semi-implicit Euler scheme. We can then iteratively produce solutions for c_k and $\nabla\phi$. If c_k is treated as a primal 0-cochain, then we must treat $c_k\nabla\phi$ as a dual 2-cochain so that we can take its divergence. This uses the following portion of the DEC-deRham diagram:

$$\begin{array}{lccc} \text{primal:} & c_k & \xrightarrow{\mathbb{D}_0} & \mathbb{D}_0 c_k \\ & & & \Big\downarrow \mathbb{M}_1 \\ \text{dual:} & (\mathbb{D}_0)^T\mathbb{M}_1\mathbb{D}_0 c_k & & \mathbb{M}_1\mathbb{D}_0 c_k \\ & (\mathbb{D}_0)^T c_k\nabla\phi & \xleftarrow[(\mathbb{D}_0)^T]{} & c_k\nabla\phi \end{array}$$

Alternatively, if c_k is treated as a dual 0-cochain, we must treat $c_k \nabla\phi$ as a primal 2-cochain and use a different portion of the diagram:

$$\begin{tikzcd}
\text{primal:} & \begin{matrix}(\mathbb{M}_2)^{-1}(\mathbb{D}_2)^T c_k \\ c_k \nabla\phi\end{matrix} \arrow[r, "\mathbb{D}_2"] & \begin{matrix}\mathbb{D}_2(\mathbb{M}_2)^{-1}(\mathbb{D}_2)^T c_k \\ \mathbb{D}_2 c_k \nabla\phi\end{matrix} \\
\text{dual:} & (\mathbb{D}_2)^T c_k \arrow[u, "(\mathbb{M}_2)^{-1}"] & c_k \arrow[l, "(\mathbb{D}_2)^T"]
\end{tikzcd}$$

An unusual aspect of (13) is that the concentration c_k is implicitly discretized differently by the two equations. In the time-dependent equation, concentration is something to which the gradient can be applied, i.e. a 0-cochain. In top equation, concentration is something which can be added to the divergence of $\vec{E}$, i.e. a 3-cochain. Thus we conclude that the discrete Hodge star operator $\mathbb{M}_0$ and its inverse must be used to transfer between the 0-cochain and 3-cochain representations of c_k during the iterative scheme. By Lemmas 4 and 5, we know that $\mathbb{M}_0^{Whit}$ and $(\mathbb{M}_0^{Dual})^{-1}$ are stable choices for this transfer. Further details of the stability analysis of electrodiffusion will be provided in the full version of this paper due to space constraints.

6. CONCLUSION

In this work we have augmented the theories of Discrete Exterior Calculus and finite element analysis by introducing two novel tools: Whitney-like interpolation functions defined on dual domain meshes and a sparse inverse discrete Hodge star. We have shown the tools to have natural, straightforward definitions and clear geometric interpretations. We have used the them to derive previously unexamined model and numerical stability criteria relating to the definition of the discrete Hodge star. Further, we have demonstrated through a variety of examples how these can and in some cases must be used to produce stable mixed finite element methods. The techniques we have described provide a valuable methodology for researchers to revisit their current finite element formulations, thereby allowing them to derive new stable discretizations of and solutions to PDEs.

Acknowledgements This research was supported in part by NIH contracts R01-EB00487, R01-GM074258, and a grant from the UT-Portugal CoLab project.

7. REFERENCES

[1] D. Arnold, R. Falk, and R. Winther. Finite element exterior calculus, homological techniques, and applications. *Acta Numerica*, pages 1–155, 2006.

[2] B. Auchmann and S. Kurz. A geometrically defined discrete hodge operator on simplicial cells. *Magnetics, IEEE Transactions on*, 42(4):643–646, April 2006.

[3] W. N. Bell. Algebraic multigrid for discrete differential forms (dissertation). Technical report, University of Illinois at Urbana-Champaign, 2008.

[4] W. N. Bell. Personal communication, 2008.

[5] A. Bossavit. Mixed finite elements and the complex of Whitney forms. In J. Whiteman, editor, *The mathematics of finite elements and applications VI*, pages 137–144. Academic Press, 1988.

[6] S. H. Christiansen. A construction of spaces of compatible differential forms on cellular complexes. *Math. Models Methods Appl. Sci.*, 18(5):739–757, 2008.

[7] M. Desbrun, A. N. Hirani, M. Leok, and J. E. Marsden. Discrete Exterior Calculus. *arXiv:math/0508341*, 2005.

[8] A. DiCarlo, F. Milicchio, A. Paoluzzi, and V. Shapiro. Discrete physics using metrized chains. In *2009 SIAM/ACM Joint Conference on Geometric and Physical Modeling*, pages 135–145. ACM, 2009.

[9] J. Dodziuk. Finite-difference approach to the Hodge theory of harmonic forms. *Amer. J. Math.*, 98(1):79–104, 1976.

[10] B. He and F. Teixeira. Geometric finite element discretization of maxwell equations in primal and dual spaces. *Physics Letters A*, 349(1-4):1 – 14, 2006.

[11] R. Hiptmair. Discrete hodge-operators: an algebraic perspective. *Progress In Electromagnetics Research*, 32:247–269, 2001.

[12] A. N. Hirani. Discrete exterior calculus (dissertation). Technical report, California Institute of Technology, 2003.

[13] A. N. Hirani, K. B. Nakshatrala, and J. H. Chaudhry. Numerical method for Darcy flow derived using Discrete Exterior Calculus. *arXiv:0810.3434*, 2008.

[14] C. L. Lopreore, T. M. Bartol, J. S. Coggan, D. X. Keller, G. E. Sosinsky, M. H. Ellisman, and T. J. Sejnowski. Computational modeling of three-dimensional electrodiffusion in biological systems: Application to the node of ranvier. *Biophysical Journal*, 95(6):2624 – 2635, 2008.

[15] P. Milbradt and T. Pick. Polytope finite elements. *International Journal for Numerical Methods in Engineering*, 73(12):1811–1835, 2008.

[16] R. Sibson. A vector identity for the Dirichlet tessellation. *Math. Proc. Cambridge Philos. Soc.*, 87(1):151–155, 1980.

[17] N. Sukumar and E. A. Malsch. Recent advances in the construction of polygonal finite element interpolants. *Archives of Computational Methods in Engineering*, 13(1):129–163, 2006.

[18] E. L. Wachspress. *A Rational Finite Element Basis*, volume 114 of *Mathematics in Science and Engineering*. Academic Press, 1975.

[19] M. Wardetzky. Discrete differential operators on polyhedral surfaces - convergence and approximation (dissertation). Technical report, Freie UniversitÃd't Berlin, 2006.

[20] H. Whitney. *Geometric Integration Theory*. Princeton University Press, 1957.

[21] S. O. Wilson. Cochain algebra on manifolds and convergence under refinement. *Topology Appl.*, 154(9):1898–1920, 2007.

[22] A. Yavari. On geometric discretization of elasticity. *Journal of Mathematical Physics*, 49(2):022901–1–36, 2008.

[23] O. Zienkiewicz and R. Taylor. *The Finite Element Method (5th edn)*. Butterworth-Heinemann, 2000.